ACCOUNTS of chemical research

Article

pubs.acs.org/accounts

Deep Eutectic Solvents: Sustainable Media for Nanoscale and Functional Materials

Durgesh V. Wagle,[†] Hua Zhao,[‡] and Gary A. Baker*[,†]

[†]Department of Chemistry, University of Missouri-Columbia, 601 South College Avenue, Columbia, Missouri 65211, United States

[‡]Department of Chemistry and Forensic Science, Savannah State University, 3219 College Street, Savannah, Georgia 31404, United States

CONSPECTUS: Deep eutectic solvents (DESs) represent an alternative class of ionic fluids closely resembling room-temperature ionic liquids (RTILs), although, strictly speaking, they are distinguished by the fact that they also contain an organic molecular component (typically, a hydrogen bond donor like a urea, amide, acid, or polyol), frequently as the predominant constituent. Practically speaking, DESs are attractive alternatives to RTILs, sharing most of their remarkable qualities (e.g., tolerance to humidity, negligible vapor pressure, thermostability, wide electrochemical potential windows, tunability) while overcoming several limitations associated with their RTIL cousins. Particularly, DESs are typically, less expensive, more synthetically accessible (typically, from bulk commodity chemicals using solvent/waste-free processes), nontoxic, and biodegradable.

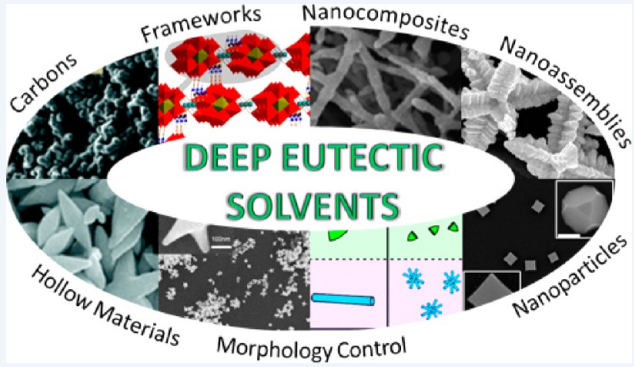

In this Account, we provide an overview of DESs as designer solvents to create well-defined nanomaterials including shape-controlled nanoparticles, electrodeposited films, metal−organic frameworks, colloidal assemblies, hierarchically porous carbons, and DNA/RNA architectures. These breakthroughs illustrate how DESs can fulfill multiple roles in directing chemistry at the nanoscale: acting as supramolecular template, metal/carbon source, sacrificial agent (e.g., ammonia release from urea), and/or redox agent, all in the absence of formal stabilizing ligand (here, solvent and stabilizer are one and the same).

The ability to tailor the physicochemical properties of DESs is central to controlling their interfacial behavior. The preorganized "supramolecular" nature of DESs provides a soft template to guide the formation of bimodal porous carbon networks or the evolution of electrodeposits. A number of essential parameters (viscosity, polarity, surface tension, hydrogen bonding), plus coordination with solutes/surfaces, all play significant roles in modulating species reactivity and mass transport properties governing the genesis of nanostructure. Furthermore, DES components may modulate nucleation and growth mechanisms by charge neutralization, modification of reduction potentials (or chemical activities), and passivation of particular crystal faces, dictating growth along preferred crystallographic directions. Broad operational windows for electrochemical reactions coupled with their inherent ionic nature facilitate the electrodeposition of alloys and semiconductors inaccessible to classical means and the use of cosolvents or applied potential control provide under-explored strategies for mediating interfacial interactions leading to control over film characteristics.

The biocompatibility of DESs suggests intriguing potential for the construction of biomolecular architectures in these novel media. It has been demonstrated that nucleic acid structures can be manipulated in the ionic, crowded, dehydrating (low water activity) DES environment—including the adoption of duplex helical structures divergent from the canonical B form and parallel G-quadruplex DNA persisting near water's boiling point—challenging the misconception that water is a necessity for maintenance of nucleic acid structure/functionality and suggesting an enticing trajectory toward DNA/RNA-based nanocatalysis within a strictly anhydrous medium.

DESs offer tremendous opportunities and open intriguing perspectives for generating sophisticated nanostructures within an anhydrous or low-water medium. We conclude this Account by offering our thoughts on the evolution of the field, pointing to areas of clear and compelling utility which will surely see fruition in the coming years. Finally, we highlight a few hurdles (e.g., need for a universal nomenclature, absence of water-immiscible, oriented-phase, and low-viscosity DESs) which, once navigated, will hasten progress in this area.

1. INTRODUCTION

The term "deep eutectic solvent" was first coined a decade ago by Abbott,[1,2] a notable pioneer in the field, who harnessed the concept of mixing two solid organic materials to yield a free-

Received: February 4, 2014
Published: June 3, 2014

   dx.doi.org/10.1021/ar5000488 | Acc. Chem. Res. 2014, 47, 2299−2308

flowing fluid with a freezing temperature far below that of either individual component. DESs are prepared by mixing high-melting-point solid organic precursors which form a liquid driven by strong hydrogen-bond interactions serving to frustrate the ability of the parent compounds to crystallize. Numerous combinations of components forming DESs by self-association of hydrogen bond donors and acceptors have been reported to date, although the most popular and well-studied examples to date involve mixtures of choline chloride with urea, ethylene glycol, or glycerol, generally in a 1:2 molar ratio.

DESs represent a nascent class of sustainable solvent and constitute a prominent addition to the repertoire of nonaqueous media being considering in green solvent engineering, among glycerol, glymes, poly(ethylene glycol), supercritical fluids, and, most particularly, room temperature ionic liquids (RTILs). Indeed, these solvents were first introduced in the context of being versatile alternatives to conventional RTILs.[1] DESs are generally obtained by mixing a quaternary ammonium halide salt like choline chloride (phosphonium-based DESs are also known) with metal salts or a hydrogen-bond donor (HBD, such as urea) capable of forming a complex with the halide ion to achieve a significant depression of the freezing point. Although DESs may fairly be considered cousins to the RTIL, albeit with a smaller ecological footprint and lower prices (facilitating scale up), some distinction between the two is in order. Namely, in point of fact, DESs are *not* RTILs in that they are not composed entirely of ions but instead have a (sometimes predominant) molecular component. Moreover, DESs are far easier (simple mixing) and cheaper to prepare, generate no waste in the process, and require no purification, aspects which embrace the Principles of Green Chemistry.

For clarity, we acknowledge that a few have recently referred to similar materials as low-transition-temperature mixtures (LTTMs) based on the notion that they display glass-phase transitions instead of melting points.[3] While we appreciate this nuanced distinction, we remain ambivalent toward such terminology for the confusion it spreads; so, for the purposes of this Account, and in practical operation, DESs are fully inclusive of LTTMs.

In this Account, we discuss prominent advances in the use of DESs to generate functional, tailored nanoscale materials. Several excellent reviews covering general aspects and properties of DESs are available,[4,5] as well as topical reviews focused on DESs are benign media for biotransformations,[6] organic synthesis,[7] biodiesel preparation,[8] and polymer synthesis;[9] interested readers are encouraged to seek them out. DESs are known to dissolve many highly polar species (e.g., metal salts, amino acids, glucose, citric acid, benzoic acid, glycerol)[1,2] and, as such, show promise for biomass processing in the dissolution of various biopolymers (lignin, chitin, cellulose, starch),[10] pretreatment of cellulosic biomass,[11,12] and glycerol removal during biodiesel synthesis.[13] Although these topics lie at the interface of materials and biology, they do not fall under the purview of this Account.

For consistency, throughout this Account, we will use the following parenthetical abbreviations for these DES systems: 1:2 choline chloride/urea (reline), 1:2 choline chloride/ethylene glycol (ethaline), and 1:2 choline chloride/glycerol (glyceline), wherein numerals denote molar ratios (Figure 1).

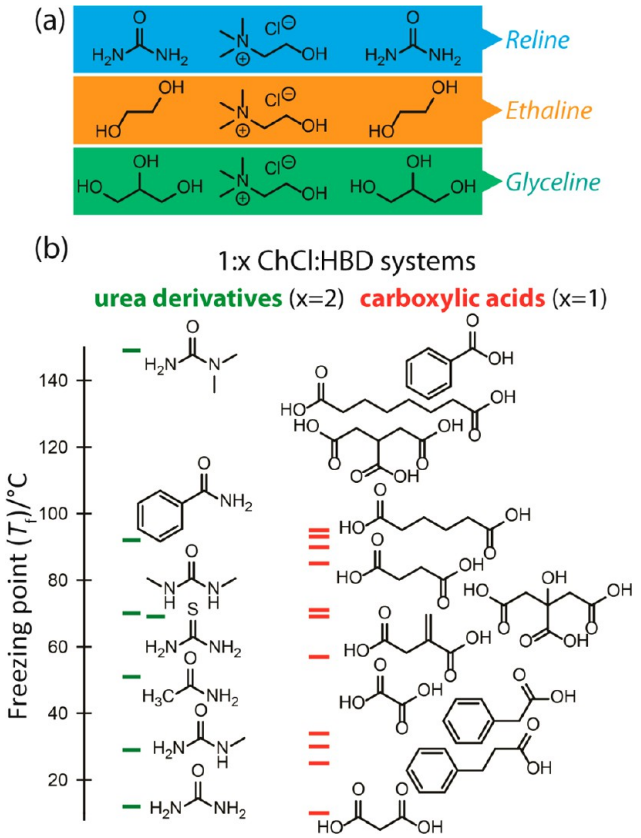

Figure 1. (a) Popular DES pairings: 1:2 choline chloride/urea (reline), 1:2 choline chloride/ethylene glycol (ethaline), and 1:2 choline chloride/glycerol (glyceline). (b) Influence of the hydrogen-bond donor (HBD) structure on experimental freezing points for DESs formed from mixtures of choline chloride/substituted ureas (1:2) and choline chloride/carboxylic acids (1:1).

2. NANOPARTICLE SYNTHESIS

2.1. Electrochemical Routes to Anisotropic Nanoparticles

Nanocrystals with high-index planes frequently exhibit activities superior to those of the most common thermodynamically stable (low-index, such as {111}, {100}, and even {110}) planes due to the presence of a high density of atomic steps, ledges, and kinks serving as active sites. Unfortunately, crystal growth rates orthogonal to a high-index plane are typically faster, so high-index planes are usually eliminated during nanocrystal growth. Indeed, it remains a challenge to synthesize well-defined nanocrystals enclosed by high-index facets.

The Sun group has contributed widely to this area, recently devising a straightforward electrochemical route to uniform ~200 nm platinum nanoflowers sporting sharp single-crystalline petals by direct electrodeposition onto a glassy carbon electrode in chloroplatinic acid (H_2PtCl_6)-containing reline at 80 °C.[14] The electrocatalytic activity of the Pt nanoflowers for ethanol oxidation in acidic solution proved to be roughly double that of commercial Pt black catalyst based on the oxidation current density. Interestingly, carrying out the synthesis at other temperatures (and thus viscosities) yielded ill-defined petals, exemplifying the delicate relationship between diffusive transport, nucleation, and growth in DESs.

Using a programmed electrodeposition method employing a square-wave potential, Sun and co-workers reported the synthesis of triambic icosahedral (TIH) Pt nanocrystals (NCs)

dx.doi.org/10.1021/ar5000488 | Acc. Chem. Res. 2014, 47, 2299−2308

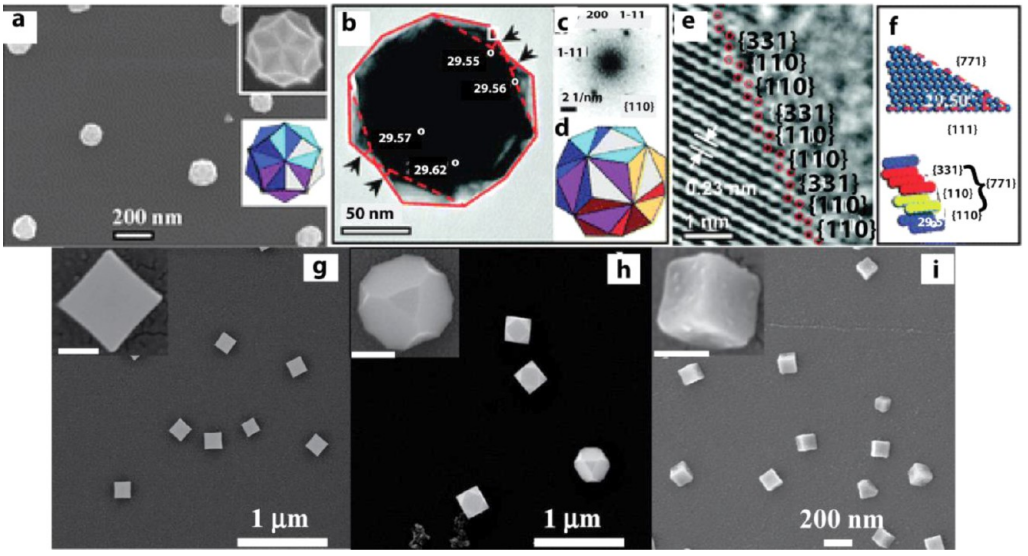

Figure 2. (a) High-magnification SEM image of triambic icosahedral (TIH) Pt NCs and a model of the TIH shape. (b) TEM image taken along the [011] direction, (c) SAED pattern, and (d) a model of the TIH Pt NC along the [011] direction which results in a 2-fold symmetry. (e) High-resolution TEM image revealing a high density of step atoms. (f) Atomic models of the Pt {771} plane. (g–i) SEM images of Pt nanostructures electrodeposited on glassy carbon in 19.3 mM H_2PtCl_6/DES solution at 80 °C for 60 min growth at different combinations of applied square-wave potentials achieving cubic, truncated cubic, and concave cubic Pt NCs. Reproduced with permission from ref 15, Copyright 2013 Royal Society of Chemistry, and ref 16, Copyright 2011 American Chemical Society.

enclosed by high-index {771} facets using reline as the solvent at 80 °C (Figure 2).[15] Along with the primary nucleation step, the interplay between the applied upper and lower limit potentials (E_U and E_L, respectively) proved crucial to NC morphogenesis; viz., truncated TIH, concave cubic, and triangular bipyramid NCs were variously formed by manipulating E_U and E_L. The control over the growth kinetics was tentatively assigned to selective and potential-dependent binding of urea to particular facets during growth.

The same fast potential cycling approach was previously used to make concave tetrahexahedral (THH) Pt NCs mainly bounded with high-index {910} and {10,1,0} facets, together with some other vicinal high-index facets of {*h*10}. The Pt NC shape and atomic arrangement (surface structure) could be varied simply by adjusting E_U and E_L as illustrated by the cubic, truncated cubic, and concave cubic Pt NCs shown in Figure 2g–i.[16] Owing to the high density of low-coordinated stepped atoms on their surfaces, THH and TIH Pt NCs exhibited enhanced catalytic activity for the electrooxidation of small organic fuels like ethanol.

Hammons et al. provided useful insight into the in situ stabilization of Pd nanoparticles (NPs) electrodeposited from reline using ultrasmall-angle X-ray scattering and electrochemical impedance spectroscopy.[17] The electrodeposited NPs were observed to assemble into two-dimensional superstructures, and the authors proposed that the adsorbate layer endowed the ensemble with a net positive charge together with induction of an anionic layer above it, although the actual surface species responsible await elucidation. This charge separation is presumably associated with a capacitance and confers colloidal stability to the assembly (i.e., upon dilution with ethanol or water, the particles readily aggregated). Importantly, the charge neutralization by the opposing ionic layer(s) in a DES represents a fundamental excursion from the simple double layer present in water wherein particle surface charges are neutralized "locally".

2.2. AntiSolvent Method

The Wong group devised a clever two-step antisolvent route to 10 nm-thick single-crystalline mesoporous ZnO nanosheets by first dissolving ZnO powders in reline at 70 °C followed by slow injection into a water bath (Figure 3, top).[18] Calcination of the recovered precipitate, which contained a mixture of wurtzite

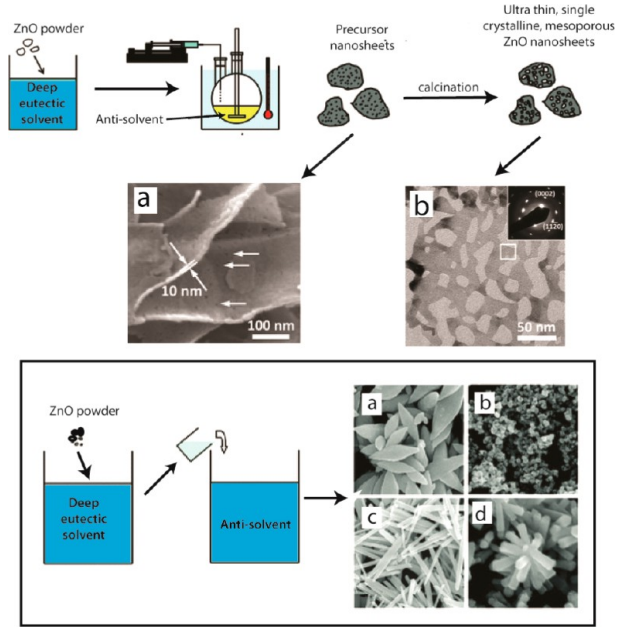

Figure 3. (Top) An antisolvent approach for the synthesis of mesoporous ZnO nanosheets. (Bottom) Schematic representing the antisolvent method for shape-controlled synthesis of varied ZnO nanostructures, including (a) twinned-cones, (b) granular particles, (c) needles, and (d) nanorod flowers. Reprinted with permission from ref 18, Copyright 2012 Royal Society of Chemistry, and ref 19, Copyright 2011 American Chemical Society.

dx.doi.org/10.1021/ar5000488 | *Acc. Chem. Res.* 2014, 47, 2299–2308

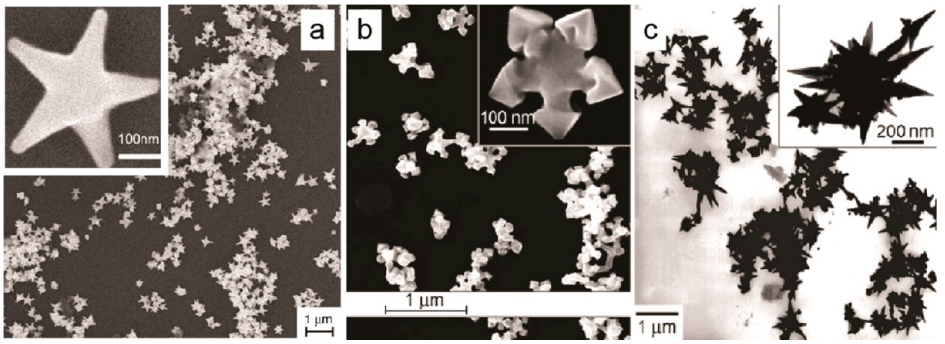

Figure 4. SEM images of (a) star-shaped and (b) snowflake-like Au NPs. (c) TEM image of Au nanothorns. Adapted with permission from ref 20. Copyright 2008 Wiley-VCH.

ZnO and $Zn_4CO_3(OH)_6{\cdot}H_2O$ phases—the latter formed by generation of carbonate and hydroxide ions derived from urea breakdown—triggered a topotactic transition involving coalescence of voids to generate larger randomly distributed pores. The calcined mesoporous ZnO nanosheets showed high specific surface areas and proved nearly as effective as commercial P-25 TiO_2 in the photocatalytic degradation of methylene blue.

The same group earlier used this antisolvent approach to demonstrate shape-controlled synthesis of crystalline ZnO nanostructures such as rice-grains, twinned-cones, granular particles, nanorods, and nanorod-corolla flowers via simple manipulation of the antisolvent composition (water−ethanol mixtures) and injection rate (Figure 3, bottom).[19] During this process, limiting the supply of ZnO by slow injection resulted in predominant crystal growth along the preferred [0001] direction, leading to the formation of well-defined nanorod structures, whereas a high degree of supersaturation led to competitive growth in less preferred directions (i.e., more isotropic growth).

2.3. Wet-Chemical Synthesis of Nanostructures

Using an expedient ambient-temperature mild reduction of $HAuCl_4$ by L-ascorbic acid (AA) in anhydrous reline, Sun and co-workers obtained ca. 300 nm polycrystalline (penta-twinned) gold star-shaped NPs bounded with {331} and vicinal high-index facets.[20] This result is remarkable in that neither seeds nor surfactant stabilizers were required. In addition to NPs exhibiting a regular pentagonal symmetry, other star-shaped Au NPs of three, four, or multiple branches were also observed and, by simply adjusting the content of water, other unique morphologies were achieved, including snowflake-like NPs and nanothorns, as shown in Figure 4. The star-shaped NPs proved to be effective electrocatalysts, with a 150 mV positive shift of the onset potential for H_2O_2 reduction plus a 14-fold enhancement in reduction current density compared to that on a polycrystalline Au electrode, an outcome attributed to the presence of high-index facets. Studying the same system, Stassi et al. showed that the polycrystalline morphology (branch formation and spiky protuberances) was highly dependent on the molar ratio of AA to $HAuCl_4$.[21]

In another example, Chirea et al. prepared polycrystalline gold nanowire networks (NWNs) by rapid $NaBH_4$-assisted reduction of $HAuCl_4$ in reline and ethaline at 40 °C.[22] The Au NWNs created in reline were shorter and wider and displayed a higher percentage of {311} facets. The generation of a higher density of low-coordinated atoms was ascribed to stronger coordination of $[AuCl_4]^-$ in reline and produced 6-fold improved catalytic activity for *p*-nitroaniline reduction over Au NWNs made in ethaline.

3. FILM ELECTRODEPOSITION

Gu et al. used a convenient galvanic replacement reaction for the electroless plating of a nanoporous Ag film on copper alloy foil from ethaline containing AgCl.[23] The bicontinuous network, the first example of nanoporous Ag film formation by galvanic replacement, was somewhat reminiscent of films produced by dealloying strategies. Surface modification by a self-assembled monolayer of *n*-dodecanethiol generated a superhydrophobic surface, the surface roughness arising from the nanoporous network playing a key role in the emergence of the "lotus effect". Quite remarkably, the same group later demonstrated the fabrication of superhydrophobic surfaces in a single step, and without any further modification, by electrodeposition of Ni films onto brass in ethaline at 90 °C.[24] In this process, the bath temperature and electrodeposition program (i.e., voltage profile, duty cycle) played important roles in deciding the final surface topology (randomly distributed nanosheets, aligned strips, or rose-shaped). For instance, higher temperatures lowered the viscosity, presumably favoring nucleation and deposition processes over growth.

Tu and co-workers electrodeposited electrochromic NiO films onto indium tin oxide in ethaline at 90 °C.[25] The higher electrodeposition temperature resulted in compact nanostructured films comprising small, uniform NPs and exhibiting favorable electrochromic properties, including a high transmittance modulation value (67%) for switching between colored and bleached states, cycling durability, and enhanced memory effects.

Taking advantage of the solubility of multiwalled carbon nanotubes (MWCNTs) in reline, Mekhalif and co-workers electrodeposited compact Ni/MWCNT composite coatings on copper substrates.[26] The MWCNTs were uniformly dispersed throughout the Ni films, and oxidized MWCNTs were found to impart higher stability and better corrosion resistance compared with their pristine counterparts, a feature ascribed to the strong affinity of nickel for oxygen.

Due to the liberation of hydrogen, electrodeposition in water is generally limited to metals with a standard reduction potential less negative than water. Nonaqueous solvents like DESs, however, can open up avenues to electronegative metals (e.g., Sm, Co, Cr, Ti, Al). Along these lines, Magagnin and co-workers realized the coelectrodeposition of Sm and Co in reline at a large negative potential (−1.6 V vs Ag/AgCl) to generate uniform, fine-grained SmCo deposits.[27] Well-defined SmCo alloy nano-

dx.doi.org/10.1021/ar5000488 | *Acc. Chem. Res.* 2014, 47, 2299−2308

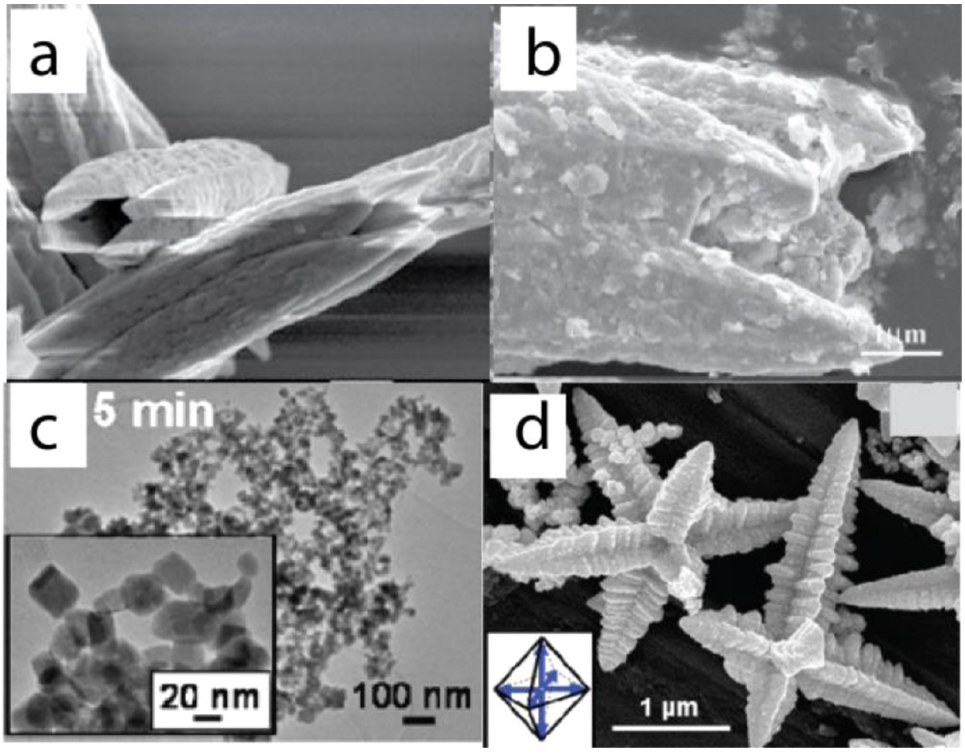

Figure 5. Various structures synthesized using ionothermal synthesis: (a) $BViO_4$ microtubules, (b) image showing the presence of nanosheets on the microtubule surface, (c) loose aggregates of PbS NCs, and (d) hierarchical hyperbranched PbS stars. Reprinted with permission from ref 30, Copyright 2010 Elsevier, and ref 31, Copyright 2012 American Chemical Society.

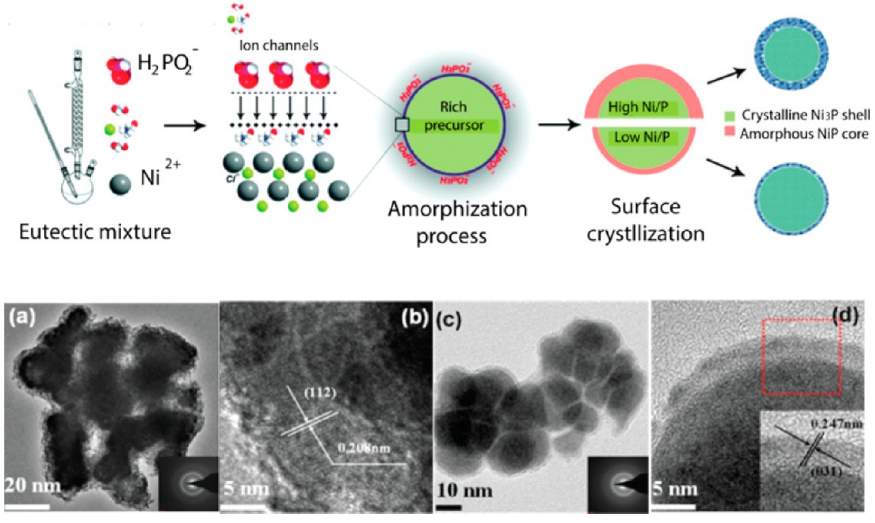

Figure 6. Schematic illustration of the synthetic procedure for the synthesis of core−shell structured NiP@Ni_3P NPs. (a−c) Representative TEM and (d) HRTEM images of the as-prepared nanomaterials. Reprinted with permission from ref 32. Copyright 2012 Royal Society of Chemistry.

wires were also grown by electrodeposition into anodic aluminum oxide membranes with uniform ∼50 nm channels.

In a striking example showing the merits of DES-based electrodeposition over industry-standard chromic acid plating, Wright et al. reported on the electrochemical deposition of highly conformal chromium coatings on individual nanotubes of vertically aligned carbon nanotube arrays using a eutectic mixture of choline chloride and $CrCl_3{\cdot}6H_2O$.[28] Employing this DES allowed the authors not only to drastically increase the current efficiency but also to carry out the deposition at much lower current densities over extended periods, yielding smooth conformal overplating of the tubes.

Studying Zn electrodeposition, Abbott and co-workers showed that additives present within the DES, such as ammonia or 1,2-diaminoethane, can exert a serious influence over the deposition mechanism and resulting film morphology.[29] More will be said on this aspect later (vide infra).

4. IONOTHERMAL SYNTHESIS

4.1. Microscale Assemblies

Liu et al. used an ionothermal treatment of bismuth nitrate and ammonium vanadate in reline at 150 °C to fabricate well-defined hollow monoclinic scheelite $BiVO_4$ microtubes 8−10 μm in

dx.doi.org/10.1021/ar5000488 | Acc. Chem. Res. 2014, 47, 2299−2308

length with dentate openings (Figure 5a,b).[30] The $BiVO_4$ microspindles showed excellent visible-light photocatalytic activity for the degradation of rhodamine B, a model pollutant fairly resistant to photocatalytic destruction.

In the most comprehensive study of nanoscale growth and self-assembly within a DES offered to date, Kotov and co-workers explored the possible formation pathways underlying the spontaneous assembly of nascent PbS nanocrystals into hyperbranched star-like superstructures (Figure 5c,d).[31] This team identified five distinct hierarchical levels in the emergence of these sophisticated superstructures: (i) formation of relatively polydisperse ca. 30 nm truncated octahedral PbS NCs and their loose agglomeration; (ii) self-assembly of 100−500 nm octahedral mesocrystals from imperfectly fused PbS NC building blocks; (iii) assembly into micrometer-scale hyperbranched star superstructures accompanied by some internal reorganization; (iv) transformation of the hyperbranched PbS stars into six-armed stars made from faceted rods; and, for prolonged reaction, (v) extensive top-down disintegration of the superstructures into shorter rods and remnant NPs.

Recently, Gu and co-workers followed an ionothermal route using ethaline to prepare core−shell NPs comprising amorphous NiP cores shelled with crystalline Ni_3P as prospective anode materials for lithium-ion batteries (Figure 6).[32] The Gu group also reported on the preparation of open-structured octahedral $Ni(NH_3)_6Cl_2$ crystals and polycrystalline α-$Ni(OH)_2$ nanoflowers using an ionothermal synthesis in reline at 150 °C.[33] Further annealing of these materials at 300 °C gave $NiCl_2$ nanosheets and mesoporous nanoflower-shaped NiO, respectively, the latter showing high specific capacitances highlighting their potential for electrical energy storage.

4.2. Open-Framework Structures

Owing to the low vapor pressure of RTILs and DESs, reactions can be conducted at temperatures well beyond 100 °C in nonpressurized vessels. In 2004, Cooper et al. introduced the concept of ionothermal synthesis which employs these fluids as dual-role solvent and structural directing agent in the synthesis of zeolite analogues.[34] These efforts have been expanded to include the ionothermal synthesis of materials with different topologies, including assorted phosphates (germanium, zirconium, aluminum), chiral materials, and metal−organic frameworks containing transition metals and lanthanides. This area has been comprehensively reviewed recently.[35,36]

5. POROUS CARBONS

DESs are gaining significant attention as media for the synthesis of porous carbons, the Gutiérrez and del Monte groups contributing extensively to the area. In early work, these researchers carried out resorcinol−formaldehyde (RF) polycondensation within ethaline followed by thermal treatment under a nonoxidative atmosphere at 800 °C to form monolithic carbons.[37] By suspending MWCNTs within the starting sol, they further showed that it was possible to achieve a remarkably homogeneous distribution of nanotubes throughout the carbon matrix.

The synthesis of hierarchically porous carbon containing both micro- and mesopores via the spinodal decomposition of tailor-made DESs based on resorcinol was also shown wherein the DES served dual roles of carbonaceous precursor and templating agent.[38] This approach gave high carbon conversions (~80%), narrow mesopore distributions, and large surface areas up to 600 $m^2\ g^{-1}$. These scientists next described the preparation of bicontinuous networks containing MWCNTs through furfuryl alcohol condensation catalyzed by a task-specific DES comprising equimolar *p*-toluenesulfonic acid and choline chloride.[39] Apart from an attractive bimodal structure with micropores plus macropores (Figure 7), the incorporation of acid-functionalized MWCNTs yielded conductive monolithic electrodes with excellent retention of the initial capacitance at high current densities.

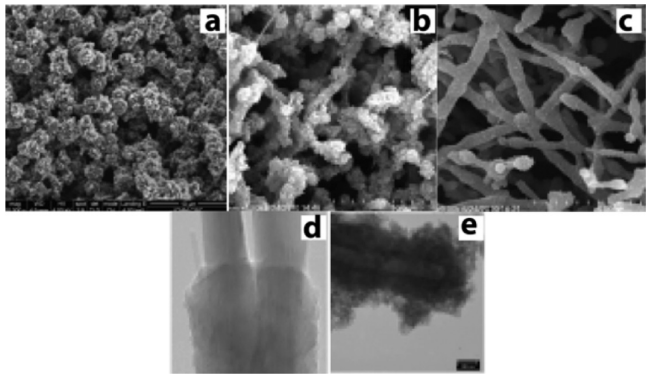

Figure 7. SEM micrographs of DES-assisted carbon derived from (a) furfuryl alcohol (FA) gel and FA gels containing (b) 13% and (c) 41% MWCNTs by weight. (d,e) TEM images of fibrillar carbon corresponding to the samples in (b) and (c), respectively. Reprinted with permission from ref 39. Copyright 2011 Wiley-VCH.

The Gutiérrez and del Monte team showed that it was possible to produce bimodally porous carbons exhibiting high surface areas (ca. 700 $m^2\ g^{-1}$) while incorporating significant nitrogen contents by RF polycondensation using DESs composed of resorcinol, 3-hydroxypyridine, and choline chloride in 1:1:1 or 2:2:1 molar ratios (Figure 8).[40] In spite of modest nitrogen

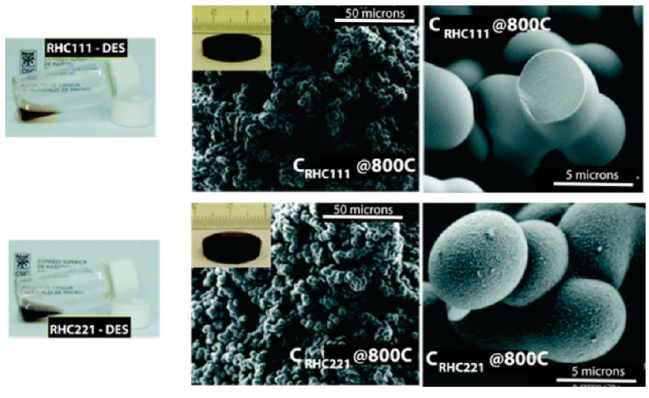

Figure 8. (Left) Pictures illustrating the free-flowing nature of DESs comprising resorcinol (R), 3-hydroxypyridine (H), and choline chloride (C) at molar rations of 1:1:1 (i.e., RHC111, top left) and 2:2:1 (RHC221, bottom left). (Right) SEM micrographs of nitrogen-doped carbons prepared via carbonization of RHC111- and RHC221-derived gels. Insets show the corresponding carbon monoliths. Reprinted with permission from ref 40. Copyright 2011 Royal Society of Chemistry.

contents, these N-doped carbons showed outstanding CO_2 sorption capacities up to 3.3 mmol g^{-1}. Similarly, carbon bimodal sorbents possessing narrow microporosity and showing outstanding selectivity for CO_2 over CH_4 were made by thermally treating RF gels obtained from a designer DES derived

from resorcinol, 4−hexylresorcinol, and tetraethylammonium bromide.[41]

Finally, Carriazo et al. described the preparation of electrically conductive carbons (up to 31 S cm^{-1}) displaying hierarchical porosity by the polycondensation of resorcinol-based DESs incorporating $Fe(CH_3CO_2)_2$, the presence of which promoted graphitization upon carbonization at moderate temperatures of 800−900 °C (Figure 9).[42]

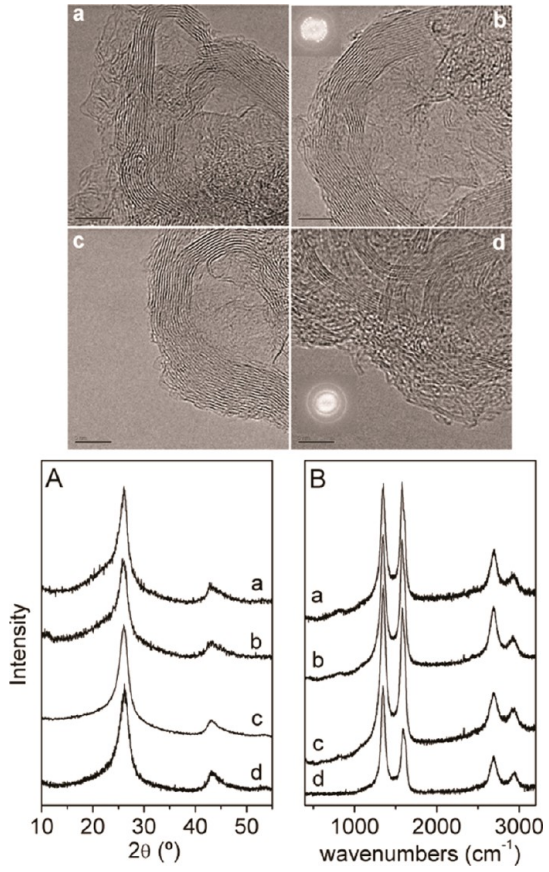

Figure 9. Graphitic carbons synthesized from DESs comprising resorcinol (R), 3-hydroxypyridine (H), urea (U), and choline chloride (C) in the presence of $Fe(CH_3CO_2)_2$. (Top) HR-TEM images of carbons prepared by thermally treating (a,b) 3.5:2:1 RUC and (c,d) 2:2:1 RHC, both at 800 °C. Scale bars are 5 nm. (Bottom) (A) XRD diffraction patterns and (B) Raman spectra of graphitic carbon derived from thermal treatment of RF gels made from (a) 3.5:2:1 RUC at 800 °C, (b) 3.5:2:1 RUC at 900 °C, (c) 2:2:1 RHC at 800 °C, and (d) 2:2:1 RHC at 900 °C. Reprinted with permission from ref 42. Copyright 2013 Wiley-VCH.

6. INTERFACIAL DES PROPERTIES MEDIATING NANOSCALE GROWTH

Given the steeply rising interest in extending DESs to materials synthesis, a fundamental insight into the mass transport and interfacial behavior (e.g., surface wetting, ionic adsorption, hydrogen bonding, double layer structure) underscoring our ability to rationally control nanoscale growth assumes great importance. While in-depth experimental and computational studies of these aspects are still awaited, several recent studies offer important preliminary insight. In one such example, the Silva group used electrochemical impedance to probe the electrochemical interface between a mercury electrode and a DES based on choline chloride plus an alkanediol or (thio)urea as HBD.[43] This study revealed that electrostatic interactions are the defining factor for the structure of the electrochemical double layer at the electrode surface which can be altered by simple electrode potential swinging; viz., positive applied potentials lead to the accumulation of anionic species as the first layer at the electrode surface, whereas choline cations dominate the interface at large negative potentials.

Much of our present understanding of DES interfacial behavior derives from electrodeposition studies. The electrodeposition of zinc in two different DESs (reline and ethaline) by Abbott et al. yielded two distinct morphologies, "rice-grains" and thin platelets, respectively.[44] Notably, the rate of deposition was higher for the more viscous reline, suggesting that the deposition of zinc in these DESs is not mass transport controlled. Electrochemical double layer differences and differences in the activity of chloride ion (which is capable of preferentially adsorbing at specific crystal faces, restricting growth in particular crystal planes) were instead suggested to be the cause of these observations. It is important to point out that, in this instance, zinc speciation itself was ruled out as a contributing factor on the basis of X-ray absorption data, which indicated that both DESs contained $[ZnCl_4]^{2-}$ as the primary species. A follow-up study from the same group demonstrated that polar additives (i.e., 0.3 M acetonitrile, ammonia, or 1,2-diaminoethane) present in the same DESs similarly exert their influence on the Zn electrodeposition mechanism by inhibition of chloride adsorption at the electrode surface to an extent determined by the hydrogen bond strength of the additive.[29]

The primary stages of electrodeposition prove to be critical as they govern the ultimate features of the deposit. In recent studies of silver electrodeposition at a platinum electrode in a DES, Abbott et al. showed that the anion controlled the silver speciation in some but not all cases.[45] The nucleation mechanism was found to be potential-dependent in this work, and it was suggested that the main factor controlling the morphology of the crystallites was the heterogeneous electron transfer rate constant—likely controlled by the strength of the metal complex in solution—which was correlated with grain size.

Xing et al. found that the surface topography of copper electrodeposited from $CuCl_2{\cdot}2H_2O$ in ethaline was strongly dependent on temperature, concentration, and electrochemical frequency.[46] These authors indicated that, by avoiding the concentration gradient near the electrode surface, pulse plating favors the formation of smooth, void-free films possessing finer and more regular grains. Proceeding from a direct current deposition to pulse plating at 50 Hz was thought to alleviate mass transport limitations, changing the deposition from a mass-controlled to a kinetically controlled one accompanied by drastic improvements in current efficiency.

The low surface tension generally associated with a DES (∼52 mN m^{-1} for reline) yields high nucleation rates, generating tiny particles which undergo Ostwald ripening only weakly. The DES solvent can play additional roles as well. For instance, a convenient room temperature route to ∼50 nm lamellar CuCl crystallites based on the reaction of $CuCl_2{\cdot}2H_2O$ and copper powder in reline was reported by Li and co-workers.[47] The DES proved to be an ideal medium for this reaction, because the $[CuCl_3]^{2-}$ complex prevailing in the chloride-rich (∼4.0 M) medium was associated with a fortuitous shift in the Cu^{2+}/Cu^{+} and Cu^{+}/Cu^{0} reduction potentials. Certainly, in water, cuprous ions are prone to disproportionation and an equivalent route is not viable.

dx.doi.org/10.1021/ar5000488 | Acc. Chem. Res. 2014, 47, 2299−2308

7. MANIPULATING NUCLEIC ACID STRUCTURE

Recent results from the Hud lab suggest that DESs may also have a role to play in the engineering of functional nucleic acid nanostructures.[48] Circular dichroism (CD) experiments performed on 32 bp mixed-sequence DNA in reline were suggestive of an A-form duplex instead of the canonical B-form helix observed in low-salt aqueous buffers, consistent with the dehydrating conditions and high ionic strength present within the DES.[48] Similarly, the inverted CD spectrum for a duplex with CG repeats ($[d(CG)_8]_2$) obtained in the same DES was indicative of a left-handed Z-form, signifying a B-to-Z-form transition. The effect is clearly sequence-dependent as both 12 bp duplex RNA and the DNA oligonucleotide $d(AT)_{16}$ exhibited similar CD spectra in the DES and in various aqueous solutions, whereas the $[d(A_4T_4)_4]_2$ duplex adopts an altered B-form helical structure (B* form) in DES. In general, the melting transition midpoints (T_M) of these DNAs in the DES are lower than their aqueous counterparts, indicating a lower duplex stability under conditions of high salt, molecular crowding, and low water activity. Intriguingly, these authors also suggested $d(A)_{16}\cdot[d(T)_{16}]_2$ triplex formation in the DES with a stability higher than the corresponding $d(A)_{16}\cdot d(T)_{16}$ duplex stability.

In other work, the Prasad group showed that ethaline and glyceline could directly dissolve salmon testes DNA at concentrations up to 5.5 and 2.5 wt %, respectively, without the need for cosolvent.[49] The DNA maintained its B-form helical structure in the DES, was chemically and structurally stable over 6 months of storage in the DES at room temperature, and could be simply recovered using cold isopropanol precipitation. In contrast, storage of the DNA in Tris buffer for the same time period resulted in biomolecular degradation, an outcome advocating DES-based chemical derivatization and/or storage media for nucleic acids.

DESs can also expand to the anhydrous environment the highly polymorphic four-stranded helices known as G-quadruplexes which are built from four guanine bases associated through Hoogsteen hydrogen bonding to form planar tetrad structures which then stack one on another. Studying short (22-mer) and long (46-mer) human telomeric DNA, as well as eight other representative G-quadruplexes in neat reline, Zhao et al. reported that the DES provided a favorable environment for the formation of unimolecular, intramolecular, and even higher-order G-quadruplexes, intriguingly with the parallel "propeller"-type topology as the preferred conformation. Extraordinarily, the construction of DNA architectures with unparalleled thermal stability is apparently possible in a DES, as these authors present examples of G-quadruplexes surviving beyond 110 °C in reline![50]

Hud and co-workers also reported that human telomere sequence (HTS) DNA adopted the parallel G-quadruplex fold in reline.[51] This supports previous conclusions that dehydration (osmotic stress) drives the formation of the parallel fold, whereas high water activity favors alternative folds. The high viscosity of the DES was shown to greatly alter the kinetics of unimolecular G-quadruplex folding on times scales ranging from minutes to months at room temperature. In particular, when thermally denatured HTS-derived oligonucleotide $d[TAG_3(TTAG_3)_3]$ (*Htelo1*) was rapidly cooled to 20 °C in the anhydrous DES, it persisted in an alternate folded state for several months before eventually folding to the thermodynamically favored parallel structure. The same experiment conducted in water required less than 2 min for refolding to occur. This behavior was suggested to be due in part to induction of kinetic trapping that is apparently inaccessible in lower-viscosity solvents like water and has gripping implications for solvent-directed "freezing" of alternate DNA folds.

8. OUTLOOK

We have provided a snapshot of the exciting progress made over the past few years employing DESs for aspects of nanoscale and functional materials synthesis, including examples in shape-controlled nanoparticle synthesis, electrodeposition, DNA manipulation, and tailored porous carbons. Given the overlap shared by the two solvent families, the exponential rise in the impact and universality of RTILs offers a roadmap for success in the field of DESs. One clear issue that arises is the need for a consensus nomenclature, an advance that helped accelerate the development of RTILs a decade ago. Indeed, the remarkable versatility of the combinations giving rise to DESs is a strength shared with RTILs; however, as Kroon and co-workers aptly point out: "the lack of standardized literature make it harder to track scientific publications in which any of them are reported."[3] Certainly, the diversity of possible combinations also resembles the early promise echoed during the embryonic growth of RTILs as a field. One key distinction, however, is that in contrast with RTILs, the number of DESs currently known which remain liquid at (and especially below) room temperature is still very limited. There is also a real need for nonpolar options which allow for formation of a juxtaposed phase with water, for liquid–liquid extractions as well as for interfacial nanoscale growth. Another unmet need is the requirement for low-viscosity alternatives to the DESs currently in use. In general, DESs are derived from cheap, abundant, nontoxic, and biodegradable natural components, limiting their thermal stabilities compared with conventional RTILs. Of course, this also makes them potentially more suited to enzyme-tolerant media and in novel bioapplications such as the liquefaction of pharmaceuticals and tissue engineering. On the whole, we predict that as our understanding of the complex interactions within DESs deepens, their relevance to nanoscience will proliferate.

■ AUTHOR INFORMATION

Corresponding Author

*E-mail: bakergar@missouri.edu.

Notes

The authors declare no competing financial interest.

Biographies

Durgesh V. Wagle is currently pursuing his Ph.D. at the University of Missouri-Columbia under the guidance of Prof. G. A. Baker. His research interests include computational chemistry and the use of deep eutectic solvents/ionic liquids in nanomaterials synthesis.

Hua Zhao studied chemistry (B.S.) and chemical engineering (M.S.) at Tianjin University (China) before earning his Ph.D. (2002) from New Jersey Institute of Technology. He completed postdoctoral training at Rutgers University. His research interests include biocatalysis in ionic liquids and deep eutectic solvents, biofuels, and microwave-assisted enzymatic reactions. He is currently Associate Professor of Chemistry and Department Chairperson at Savannah State University.

Gary A. Baker received his Ph.D. in Analytical Chemistry from the University of Buffalo under the direction of Frank V. Bright. After postdoctoral training at Los Alamos National Laboratory with T. Mark McCleskey, followed by a staff position at Oak Ridge National Laboratory, he began his independent academic career at the University

of Missouri-Columbia in 2011 where his research interests include nanoenabled sustainable energy, ionic liquids, and deep eutectic solvents.

■ ACKNOWLEDGMENTS

We thank the ACS PRF program for their support of work related to that discussed herein. GAB dedicates this review to the loving memory of Beulah Rose Baker (1949−2012): *a guiding light gone far too soon.*

■ REFERENCES

(1) Abbott, A. P.; Boothby, D.; Capper, G.; Davies, D. L.; Rasheed, R. K. Deep Eutectic Solvents Formed Between Choline Chloride and Carboxylic Acids: Versatile Alternatives to Ionic Liquids. *J. Am. Chem. Soc.* **2004**, *126*, 9142−9147.

(2) Abbott, A. P.; Capper, G.; Davies, D. L.; Rasheed, R. K.; Tambyrajah, V. Novel Solvent Properties of Choline Chloride/Urea Mixtures. *Chem. Commun.* **2003**, 70−71.

(3) Francisco, M.; Van Den Bruinhorst, A.; Kroon, M. C. Low-Transition-Temperature Mixtures (LTTMs): A New Generation of Designer Solvents. *Angew. Chem., Int. Ed.* **2013**, *52*, 3074−3085.

(4) Zhang, Q.; De Oliveira Vigier, K.; Royer, S.; Jerome, F. Deep Eutectic Solvents: Syntheses, Properties and Applications. *Chem. Soc. Rev.* **2012**, *41*, 7108−7146.

(5) Tang, S.; Baker, G. A.; Zhao, H. Ether- and Alcohol-Functionalized Task-Specific Ionic Liquids: Attractive Properties and Applications. *Chem. Soc. Rev.* **2012**, *41*, 4030−4066.

(6) Domínguez de María, P.; Maugeri, Z. Ionic Liquids in Biotransformations: From Proof-Of-Concept to Emerging Deep-Eutectic-Solvents. *Curr. Opin. Chem. Biol.* **2011**, *15*, 220−225.

(7) Ruß, C.; König, B. Low Melting Mixtures in Organic Synthesis − An Alternative to Ionic Liquids? *Green Chem.* **2012**, *14*, 2969−2982.

(8) Zhao, H.; Baker, G. A. Ionic Liquids and Deep Eutectic Solvents for Biodiesel Synthesis: A Review. *J. Chem. Technol. Biotechnol.* **2013**, *88*, 3−12.

(9) Carriazo, D.; Serrano, M. C.; Gutierrez, M. C.; Ferrer, M. L.; del Monte, F. Deep-Eutectic Solvents Playing Multiple Roles in the Synthesis of Polymers and Related Materials. *Chem. Soc. Rev.* **2012**, *41*, 4996−5014.

(10) Sharma, M.; Mukesh, C.; Mondal, D.; Prasad, K. Dissolution of α-Chitin in Deep Eutectic Solvents. *RSC Adv.* **2013**, *3*, 18149−18155.

(11) Francisco, M.; van den Bruinhorst, A.; Kroon, M. C. New Natural and Renewable Low Transition Temperature Mixtures (LTTMs): Screening as Solvents for Lignocellulosic Biomass Processing. *Green Chem.* **2012**, *14*, 2153−2157.

(12) Xia, S.; Baker, G. A.; Li, H.; Ravula, S.; Zhao, H. Aqueous Ionic Liquids and Deep Eutectic Solvents for Cellulosic Biomass Pretreatment and Saccharification. *RSC Adv.* **2014**, *4*, 10586−10596.

(13) Abbott, A. P.; Cullis, P. M.; Gibson, M. J.; Harris, R. C.; Raven, E. Extraction of Glycerol from Biodiesel into a Eutectic Based Ionic Liquid. *Green Chem.* **2007**, *9*, 868−872.

(14) Wei, L.; Fan, Y.-J.; Wang, H.-H.; Tian, N.; Zhou, Z.-Y.; Sun, S.-G. Electrochemically Shape-Controlled Synthesis in Deep Eutectic Solvents of Pt Nanoflowers with Enhanced Activity for Ethanol Oxidation. *Electrochim. Acta* **2012**, *76*, 468−474.

(15) Wei, L.; Zhou, Z.-Y.; Chen, S.-P.; Xu, C.-D.; Su, D.; Schuster, M. E.; Sun, S.-G. Electrochemically Shape-Controlled Synthesis in Deep Eutectic Solvents: Triambic Icosahedral Platinum Nanocrystals with High-Index Facets and Their Enhanced Catalytic Activity. *Chem. Commun.* **2013**, *49*, 11152−11154.

(16) Wei, L.; Fan, Y.-J.; Tian, N.; Zhou, Z.-Y.; Zhao, X.-Q.; Mao, B.-W.; Sun, S.-G. Electrochemically Shape-Controlled Synthesis in Deep Eutectic Solvents—A New Route to Prepare Pt Nanocrystals Enclosed by High-Index Facets with High Catalytic Activity. *J. Phys. Chem. C* **2011**, *116*, 2040−2044.

(17) Hammons, J. A.; Muselle, T.; Ustarroz, J.; Tzedaki, M.; Raes, M.; Hubin, A.; Terryn, H. Stability, Assembly, and Particle/Solvent Interactions of Pd Nanoparticles Electrodeposited from a Deep Eutectic Solvent. *J. Phys. Chem. C* **2013**, *117*, 14381−14389.

(18) Dong, J.-Y.; Lin, C.-H.; Hsu, Y.-J.; Lu, S.-Y.; Wong, D. S.-H. Single-Crystalline Mesoporous ZnO Nanosheets Prepared with a Green Antisolvent Method Exhibiting Excellent Photocatalytic Efficiencies. *CrystEngComm* **2012**, *14*, 4732−4737.

(19) Dong, J.-Y.; Hsu, Y.-J.; Wong, D. S.-H.; Lu, S.-Y. Growth of ZnO Nanostructures with Controllable Morphology Using a Facile Green Antisolvent Method. *J. Phys. Chem. C* **2010**, *114*, 8867−8872.

(20) Liao, H.-G.; Jiang, Y.-X.; Zhou, Z.-Y.; Chen, S.-P.; Sun, S.-G. Shape-Controlled Synthesis of Gold Nanoparticles in Deep Eutectic Solvents for Studies of Structure−Functionality Relationships in Electrocatalysis. *Angew. Chem., Int. Ed.* **2008**, *47*, 9100−9103.

(21) Stassi, S.; Cauda, V.; Canavese, G.; Manfredi, D.; Pirri, C. F. Synthesis and Characterization of Gold Nanostars as Filler of Tunneling Conductive Polymer Composites. *Eur. J. Inorg. Chem.* **2012**, *2012*, 2669−2673.

(22) Chirea, M.; Freitas, A.; Vasile, B. S.; Ghitulica, C.; Pereira, C. M.; Silva, F. Gold Nanowire Networks: Synthesis, Characterization, and Catalytic Activity. *Langmuir* **2011**, *27*, 3906−3913.

(23) Gu, C. D.; Xu, X. J.; Tu, J. P. Fabrication and Wettability of Nanoporous Silver Film on Copper from Choline Chloride-Based Deep Eutectic Solvents. *J. Phys. Chem. C* **2010**, *114*, 13614−13619.

(24) Gu, C.; Tu, J. One-Step Fabrication of Nanostructured Ni Film with Lotus Effect from Deep Eutectic Solvent. *Langmuir* **2011**, *27*, 10132−10140.

(25) Cai, G.-f.; Tu, J.-p.; Gu, C.-d.; Zhang, J.-h.; Chen, J.; Zhou, D.; Shi, S.-j.; Wang, X.-l. One-Step Fabrication of Nanostructured NiO Films from Deep Eutectic Solvent with Enhanced Electrochromic Performance. *J. Mater. Chem. A* **2013**, *1*, 4286−4292.

(26) Martis, P.; Dilimon, V. S.; Delhalle, J.; Mekhalif, Z. Electro-Generated Nickel/Carbon Nanotube Composites in Ionic Liquid. *Electrochim. Acta* **2010**, *55*, 5407−5410.

(27) Gomez, E.; Valles, E.; Cojocaru, P.; Raygani, A.; Magagnin, L. Electrodeposition of SmCo Nanostructures in Deep Eutectic Solvent. *ECS Trans.* **2012**, *41*, 3−9.

(28) Wright, A. C.; Faulkner, M. K.; Harris, R. C.; Goddard, A.; Abbott, A. P. Nanomagnetic Domains of Chromium Deposited on Vertically-Aligned Carbon Nanotubes. *J. Magn. Magn. Mater.* **2012**, *324*, 4170−4174.

(29) Abbott, A. P.; Barron, J. C.; Frisch, G.; Ryder, K. S.; Silva, A. F. The Effect of Additives on Zinc Electrodeposition from Deep Eutectic Solvents. *Electrochim. Acta* **2011**, *56*, 5272−5279.

(30) Liu, W.; Yu, Y.; Cao, L.; Su, G.; Liu, X.; Zhang, L.; Wang, Y. Synthesis of Monoclinic Structured $BiVO_4$ Spindly Microtubes in Deep Eutectic Solvent and Their Application for Dye Degradation. *J. Hazard. Mater.* **2010**, *181*, 1102−1108.

(31) Querejeta-Fernández, A.; Hernández-Garrido, J. C.; Yang, H.; Zhou, Y.; Varela, A.; Parras, M.; Calvino-Gámez, J. J.; González-Calbet, J. M.; Green, P. F.; Kotov, N. A. Unknown Aspects of Self-Assembly of PbS Microscale Superstructures. *ACS Nano* **2012**, *6*, 3800−3812.

(32) Zhang, H.; Lu, Y.; Gu, C.-D.; Wang, X.-L.; Tu, J.-P. Ionothermal Synthesis and Lithium Storage Performance of Core/Shell Structured Amorphous@crystalline Ni-P Nanoparticles. *CrystEngComm* **2012**, *14*, 7942−7950.

(33) Ge, X.; Gu, C. D.; Lu, Y.; Wang, X. L.; Tu, J. P. A Versatile Protocol for the Ionothermal Synthesis of Nanostructured Nickel Compounds as Energy Storage Materials from a Choline Chloride-Based Ionic Liquid. *J. Mater. Chem. A* **2013**, *1*, 13454−13461.

(34) Cooper, E. R.; Andrews, C. D.; Wheatley, P. S.; Webb, P. B.; Wormald, P.; Morris, R. E. Ionic Liquids and Eutectic Mixtures as Solvent and Template in Synthesis of Zeolite Analogues. *Nature* **2004**, *430*, 1012−1016.

(35) Morris, R. E. Ionothermal Synthesis-Ionic Liquids as Functional Solvents in the Preparation of Crystalline Materials. *Chem. Commun.* **2009**, 2990−2998.

(36) Parnham, E. R.; Morris, R. E. Ionothermal Synthesis of Zeolites, Metal−Organic Frameworks, and Inorganic−Organic Hybrids. *Acc. Chem. Res.* **2007**, *40*, 1005−1013.

(37) Gutiérrez, M. C.; Rubio, F.; del Monte, F. Resorcinol-Formaldehyde Polycondensation in Deep Eutectic Solvents for the Preparation of Carbons and Carbon−Carbon Nanotube Composites. *Chem. Mater.* **2010**, *22*, 2711−2719.
(38) Carriazo, D.; Gutiérrez, M. C.; Ferrer, M. L.; del Monte, F. Resorcinol-Based Deep Eutectic Solvents as Both Carbonaceous Precursors and Templating Agents in the Synthesis of Hierarchical Porous Carbon Monoliths. *Chem. Mater.* **2010**, *22*, 6146−6152.
(39) Gutiérrez, M. C.; Carriazo, D.; Tamayo, A.; Jiménez, R.; Picó, F.; Rojo, J. M.; Ferrer, M. L.; del Monte, F. Deep-Eutectic-Solvent-Assisted Synthesis of Hierarchical Carbon Electrodes Exhibiting Capacitance Retention at High Current Densities. *Chem.—Eur. J.* **2011**, *17*, 10533−10537.
(40) Gutierrez, M. C.; Carriazo, D.; Ania, C. O.; Parra, J. B.; Ferrer, M. L.; del Monte, F. Deep Eutectic Solvents as Both Precursors and Structure Directing Agents in the Synthesis of Nitrogen Doped Hierarchical Carbons Highly Suitable for CO_2 Capture. *Energy Environ. Sci.* **2011**, *4*, 3535−3544.
(41) Patino, J.; Gutierrez, M. C.; Carriazo, D.; Ania, C. O.; Parra, J. B.; Ferrer, M. L.; del Monte, F. Deep Eutectic Assisted Synthesis of Carbon Adsorbents Highly Suitable for Low-Pressure Separation of CO_2−CH_4 Gas Mixtures. *Energy Environ. Sci.* **2012**, *5*, 8699−8707.
(42) Carriazo, D.; Gutiérrez, M. C.; Jiménez, R.; Ferrer, M. L.; del Monte, F. Deep-Eutectic-Assisted Synthesis of Bimodal Porous Carbon Monoliths with High Electrical Conductivities. *Part. Part. Syst. Charact.* **2013**, *30*, 316−320.
(43) Costa, R.; Figueiredo, M.; Pereira, C. M.; Silva, F. Electrochemical Double Layer at the Interfaces of Hg/Choline Chloride Based Solvents. *Electrochim. Acta* **2010**, *55*, 5.
(44) Abbott, A. P.; Barron, J. C.; Frisch, G.; Gurman, S.; Ryder, K. S.; Fernando Silva, A. Double Layer Effects on Metal Nucleation in Deep Eutectic Solvents. *Phys. Chem. Chem. Phys.* **2011**, *13*, 10224−10231.
(45) Abbott, A. P.; Azam, M.; Frisch, G.; Hartley, J.; Ryder, K. S.; Saleem, S. Ligand Exchange in Ionic Systems and its Effect on Silver Nucleation and Growth. *Phys. Chem. Chem. Phys.* **2013**, *15*, 17314−17323.
(46) Xing, S.; Zanella, C.; Deflorian, F. Effect of Pulse Current on the Electrodeposition of Copper from Choline Chloride-Ethylene Glycol. *J. Solid State Electrochem.* **2014**, 1−7.
(47) Zhang, F.; Lai, J.; Huang, Y.; Li, F.; Luo, G.; Chu, G. A Green Method for Preparing CuCl Nanocrystal in Deep Eutectic Solvent. *Aust. J. Chem.* **2013**, *66*, 237−240.
(48) Mamajanov, I.; Engelhart, A. E.; Bean, H. D.; Hud, N. V. DNA and RNA in Anhydrous Media: Duplex, Triplex, and G-Quadruplex Secondary Structures in a Deep Eutectic Solvent. *Angew. Chem., Int. Ed.* **2010**, *49*, 6310−6314.
(49) Mondal, D.; Sharma, M.; Mukesh, C.; Gupta, V.; Prasad, K. Improved Solubility of DNA in Recyclable and Reusable Bio-Based Deep Eutectic Solvents with Long-Term Structural and Chemical Stability. *Chem. Commun.* **2013**, *49*, 9606−9608.
(50) Zhao, C.; Ren, J.; Qu, X. G-Quadruplexes Form Ultrastable Parallel Structures in Deep Eutectic Solvent. *Langmuir* **2013**, *29*, 1183−1191.
(51) Lannan, F. M.; Mamajanov, I.; Hud, N. V. Human Telomere Sequence DNA in Water-Free and High-Viscosity Solvents: G-Quadruplex Folding Governed by Kramers Rate Theory. *J. Am. Chem. Soc.* **2012**, *134*, 15324−15330.